The Relative Stabilities of Base Pair Stacking Interactions and Single Mismatches in Long RNA Measured by Temperature Gradient Gel Electrophoresis†

Jian Zhu and Roger M. Wartell*

School of Biology, Georgia Institute of Technology, Atlanta, Georgia 30332

Received July 10, 1997; Revised Manuscript Received September 22, 1997⊗

ABSTRACT: The thermal stability of RNA duplexes differing by a single base pair (bp) substitution or mismatch were investigated by temperature gradient gel electrophoresis (TGGE). All base pair substitutions and mismatches were examined at six sites, and limited changes were investigated at three other sites. DNA templates for in vitro transcription were generated by the polymerase chain reaction (PCR). Transcribed forward and reverse single stranded RNAs were annealed to form 345 bp dupex RNA. Solution melting curves of selected RNAs were in good agreement with the predicted three step transitions. Parallel TGGE was used to determine the relative stabilities of the RNAs, and perpendicular TGGE was employed to obtain mobility transitions and midpoint transition temperatures (T_μ) of the RNAs' first melting domain. The gel solvent included formamide and urea. The T_μ values of the first melting domain were influenced by the identity of the base pair substitution or mismatch as well as by the site's neighboring base pairs. The difference in the transition temperatures (δT_μ) between pairs of RNA ranged from 0 to 5 °C. δT_μ values were used to determine free energy differences ($\delta\Delta G$). For RNA pairs distinguished by a base pair substitution, the $\delta\Delta G$ values were closely correlated with free energy differences calculated from stacking free energies determined from melting studies in 1 M Na^+ [Serra, M. J., and Turner, D. H. (1995) *Methods Enzymol. 259*, 242−261.] An algorithm was developed using the free energies of terminal mismatches [Serra, M. J., and Turner, D. H. (1995) *Methods Enzymol. 259*, 242−261] that provided very good agreement with experimental free energies for the single internal mismatches.

The investigation of structure/function relationships of RNA molecules often rely on the prediction of RNA secondary structure from the primary sequence. The most successful algorithms for predicting RNA secondary structure seek the lowest free energy structure based on free energy increments of subfragment structural motifs. Common motifs include duplex segments, hairpin loops, and duplex segments with mismatches, bulges, or dangling ends. The free energy increment for duplex base pairs has been empirically determined from the analysis of short RNA duplex melting curves (*1*−*3*). The effects of 3′ and 5′ dangling nucleotides and terminal mismatches at a duplex end have also been evaluated (*3*). The free energy increments for single internal mismatches are not well-known. Although the stabilities of a variety of tandem mismatches have been evaluated (*4*), the properties of a single mismatch may not be simply related to its tandem form. The effects of single and tandem purine mismatches on the stability of short RNA duplexes indicate that interactions beyond nearest neighbor base pairs can occur (*5*).

In this study, temperature gradient gel electrophoresis (TGGE)[1] was employed to evaluate the effects of single base pair changes and mismatches on the stability of a 345 base pair (bp) RNA duplex. Duplex RNAs differing in stability in their first melting domain unwind and decrease in mobility at different depths in a polyacrylamide gel with a superimposed temperature gradient. The separation can be quantitatively measured with temperature gradients superimposed either parallel or perpendicular to the direction of mobility. TGGE has been previously employed to detect mutations in DNA (*6*) and to evaluate the relative stabilities of PCR-generated defects in DNA (i.e., single mismatches, base bulges, and tandem mismatches (*7, 8, 9*).

Using PCR amplification and in vitro transcription, we have now extended the latter approach to RNA. The method provides a new approach for evaluating the relative stability of RNA structural motifs. The relative stabilities of all base pair stacking interactions and single mismatches at six different positions in a RNA duplex were determined. A limited number of base pair changes were produced at three other sites. The free energy differences of base pair stacking interactions evaluated from the TGGE approach were in very good agreement with available thermodynamic data obtained from UV absorbance melting curves, despite the significant differences in solvents and systems employed. A set of simple rules was established that was able to relate the free energy differences of previously obtained data on terminal RNA mismatches with single internal mismatches measured by TGGE. These rules may be useful in secondary structure predictions of RNA (*10, 11*).

MATERIALS AND METHODS

TGGE. Temperature gradient gel electrophoresis was carried out with a vertical slab-gel apparatus that has been previously described (*13*). The glass plates containing the polyacrylamide gel was sandwiched by two aluminum heating blocks that established a temperature gradient either parallel or perpendicular to the direction of electrophoresis.

† This work was supported by the Emory-Georgia Tech Biomedical Research Center

* Author to whom correspondence should be addressed.

⊗ Abstract published in *Advance ACS Abstracts,* November 15, 1997.

[1] Abbreviations: TGGE, temperature gradient gel electrophoresis; PCR, polymerase chain reaction.

S0006-2960(97)01678-4 CCC: $14.00

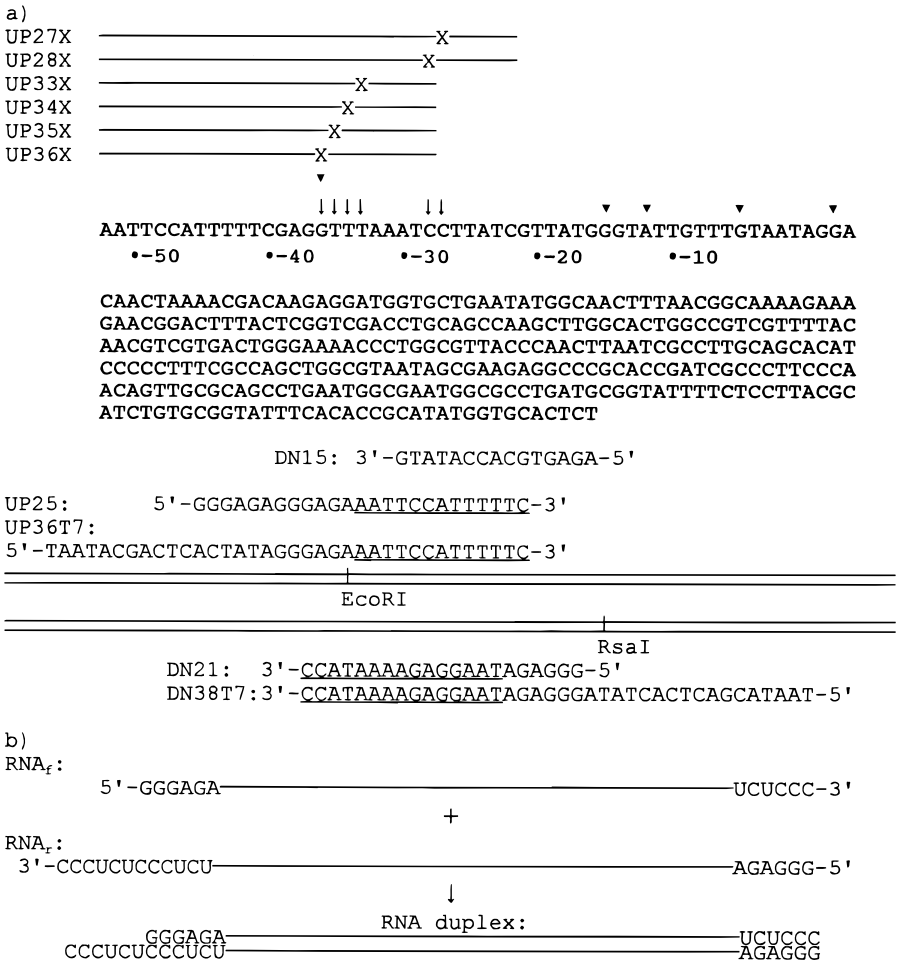

FIGURE 1: (a) The 373 bp DNA region of pUC8-31 numbered relative to the *ctc* promoter startpoint. Plasmids pUC8-5, pUC-12, pUC-15, and pUC-36 have base pair differences from pUC8-31 at positions −5 (G to A), −12 (A to T), −15 (G to A), and −36 (G to A) respectively (indicated by ▼). PCR was used with upstream primers (UP27X to UP36X, X = A, T, G or C) to generate DNA fragments with all possible base pairs at positions indicated by down arrows (↓). A common downstream primer (DN15) was employed. The resulting PCR products or plasmids were used as templates for a second round of PCR. Two sets of primers were used to add a T7 promoter sequence on one or the other end of each DNA product. The primers that generated the "forward" transcription template were UP36T7 and DN21. For the "reverse" template, the primer pair was DN38T7 and UP25. Underlined bases were complementary to the initial template. (b) The transcription templates from part a were used to produce RNA_f (345 nt) and RNA_r (351 nt). When hybridized, the RNA strands formed a 345 bp duplex with a 6 base tail on the 3′ strand at the EcoR I end.

A 6.5% polyacrylamide gel (acrylamide:bisacrylamide, 37.5:1) was used. The gel solution contained 0.5X TBE, pH 8.3 (0.045 M Tris + 0.045 M boric acid + 2 mM EDTA), and the denaturants 4.06 M urea and 23.3% (v/v) formamide. The latter corresponds to 58% of the 100% denaturant solution (7 M urea + 40% formamide). Formamide was deionized with BioRad Inc. mixed resin AG501-X8D and stored at −20 °C. The electrophoresis buffer was 0.5X TBE (pH 8.3). Procedures for obtaining DNA mobility curves from perpendicular TGGE gel images were as previously described (*7, 8*).

DNA Plasmids and Fragments. DNA fragments employed as templates for RNA transcription were produced by PCR from five related plasmids and a group of related DNA fragments. The plasmids contained a 130 bp insert of the *ctc* promoter region from *Bacillus subtilus* between the *Hin*dIII and *Eco*RI sites of the pUC8 plasmid (*11*). The four plasmids, pUC8-5, pUC8-12, pUC8-15, and pUC8-36, had single base pair differences from the wild type sequence, pUC8-31, in the 373 bp region between the *Eco*RI and *Rsa*I restriction endonuclease sites. The wild type sequence of this region is given in Figure 1. Each of the other plasmids had a GC to AT substitution except for pUC8-12, which had an AT to TA substitution. The five filled triangles in Figure 1 show the location of the base pair changes in the 373 bp sequence of the plasmids. Except for pUC8-31, the suffix designation of each plasmid, e.g. -5′, refers to the location of the base pair change relative to the transcription startpoint of the *ctc* promoter. In addition to the six plasmid DNAs, deoxyribonucleotide primers were used to produce 19 DNA fragments, 373 bp long, with all possible base pairs (AT, TA, GC, and CG) at positions −36, −35, −34, −33, −28, and −27, respectively. The wild type plasmid, pUC8-31, was used as a PCR template to generate these fragments.

Transcription Templates. PCR-generated DNA templates for in vitro transcription were prepared from the purified plasmids and PCR-produced 373 bp DNA fragments. The primers in these reactions added a T7 promoter sequence on one end or the other of each resultant DNA. The primers employed to generate the "forward" DNA template were a 36-base oligomer, UP36T7 (5′-TAATACGACTCACTATAGGGAGAAATTCCATTTTTC-3′), and a 21-base oligomer, DN21 (5′GGGAGATAAGGAGAAAATACC-3′). The underlined bases indicate the sequence complimentary to the initial template. For the "reverse" DNA template, the primer pair consisted of a 38-base oligomer, DN38T7 (5′-TAATAC-

GACT CACTATAGGGAGATAAGGAGAAAATACC-3′) and a 25 base oligomer, UP25 (5′-GGGAGAGGGAGAAATTCCATTTTTC-3′). Figure 1a shows the approximate location of the above primers relative to the *Eco*RI and *Rsa*I end sites of the 373 bp DNA sequence. Figure 1b shows RNA_f and RNA_r, the forward and reverse transcripts, respectively. When hybridized, the RNA strands formed a 345 bp duplex with a 6 base tail on the 3′ strand at the *Eco*RI end. These RNAs were used in the TGGE and UV melting studies.

PCR Conditions. All polymerase chain reactions employed a volume of 100 μL with a buffer of 10 mM Tris (pH 8.3), 50 mM KCl, 2 mM $MgCl_2$, 0.6 μM of each primer, and 0.2 mM of each dNTP. An additional 0.2 mM dATP was often added to the reaction in order to obtain a single DNA band on a temperature gradient gel (described below). The initial reactions for generating base pair substitutions at specific sites contained 100 pg of purified pUC8-31 plasmid as template. PCR products from these reactions that were used to template a second round of PCR were purified by running 3 μL of a reaction on a 6% polyacrylamide gel PAG, cutting out the relevant DNA band, and eluting the DNA fragment overnight in 50 μL of 10 mM Tris and 1 mM EDTA. PCR mixtures were overlaid with 100 μL of mineral oil, placed in a thermal cycler, and held at 80 °C for 10 min before the addition of 2.5 units of Taq DNA polymerase (Promega or BRL). The reaction mixture was subjected to 35 cycles of denaturation at 94 °C for 1 min, primer annealing at 55 °C for 1 min, and primer extension at 72 °C for 2 min. An additional 5 min incubation at 72 °C allowed for the completion of primer extension after the last cycle.

PCR products were first characterized on a 6% polyacrylamide gel and exhibited a single DNA band by ethidium bromide staining. However, when a PCR product, synthesized with equimolar amounts of dNTPs, was further examined with a parallel temperature gradient gel, two closely spaced DNA bands were observed. The gradient was from 30−35 °C. This occurred using plasmid or fragment templates. When an additional 0.2 mM dATP was employed in the PCR, the products showed only one major band after electrophoresis in a temperature gradient gel. It has been shown that Taq DNA polymerase can add from one to a few nontemplate-directed nucleotides to a blunt-ended duplex DNA fragment, and it preferably adds dATP (*14*). We hypothesized that in the PCR with equimolar dNTPs, some product DNAs carried an extra A at the duplex ends. The blunt-ended DNA and base-extended DNA may have slightly differing stabilities, which would produce doublet bands by TGGE. The extra 0.2 mM dATP may have saturated the reaction causing A-additions since a single major band was observed for these PCR products.

In Vitro Transcription. All solutions relating to RNA production and processing were prepared with diethyl pyrocarbonate (DEPC) treated water according to methods described by Sambrook et al. (*15*). The forward and reverse RNAs were synthesized from the PCR-generated templates described in Figure 1b. PCR products used for transcription were either purified by a phenol−chloroform extraction followed by ethanol precipitation or used directly. For a 20 μL reaction, approximately 0.1 μg of purified DNA template or 8 μL of the unpurified PCR product was used in a 20 μL reaction. RNA yields were similar for both cases. The reaction mixture contained 8 mM Tris-HCl (pH 8.0), 6 mM $MgCl_2$, 10 mM NaCl, 2 mM spermidine, 1 mM DTT, 1 unit RNase inhibitor (5′ → 3′ Inc.), 1 mM of each rNTP, and 10 units T7 RNA polymerase (Epicenter Technologies Inc). The reaction was carried out at 37 °C for 2 h. At the end of the reaction, 1 μL of the reaction mixture was mixed with 4 μL of formamide and loaded on a 6% PAG with 7 M urea. Ethidium bromide staining was used to visualize the RNA produced. After this verification of the reaction, 2 units of RNase free DNase (Promega) was added to the reaction mixture. The digestion was carried out for 15 min at 37 °C and stopped by phenol−chloroform extraction.

The RNA duplexes employed in our studies carried six nucleotide (3′-UCUCCC-5′) extension on the 3′ end of the lowest melting domain. This extra tail was added to counteract the ability of T7 RNA polymerase to add nontemplated bases at the end of a RNA transcript in a runoff transcription reaction (*15*). TGGE is sufficiently sensitive that it can apparently detect the effect of unpaired bases at the end of the lowest melting domain (see above). In order to minimize this end effect, the six nucleotide tail was attached to the RNA duplex to move the heterogeniety of the ends further from the base paired domain. T7 polymerase can still add an extra base or two at the end of the tail, but the added bases are expected to have a smaller effect on the stability of the duplex. The RNAs carrying the 3′ tail showed single bands in parallel TGGE experiments; however, the RNAs without this tail showed several well-separated bands (not shown).

Approximately equimolar amounts of the forward transcript (designated as f) and reverse transcript (designated as r) were mixed to form the desired RNA duplexes. The mixture was held at 90 °C for 3 min and kept at 60 °C for 30 min followed by a 1 h incubation at 37 °C. The visual intensity of ethidium bromide stained gel bands of complimentary RNA strands were used to determine if the concentrations of the f and r strands were approximately equal. Although this sometimes resulted in a slight excess of one strand over the other, the excess strand did not interfere with the gel melting behavior of the duplex. The extra RNA band was always well-separated from the double-stranded (ds) RNA in the polyacrylamide gels. In parallel TGGE experiments, 3 μL of the ds RNA samples (0.5−1.0 μg) were loaded in each lane with 1 μL of loading buffer (30% Ficol). The temperature gradient was 5 or 6 °C between 34 and 45 °C. The running time was 14−16 h. For perpendicular TGGE, 15 μL of the RNA duplex (∼5 μg) was loaded. The temperature gradient was from a minimum of 20 °C to a maximum of 55−60 °C. The running time was 12−16 h. RNA duplexes are designated in the text by the base pair position being investigated (referenced to Figure 1a), followed by the base pair or mismatch at the position. For example, (−27AC) represents the RNA carrying an AC mismatch at position −27.

Melting Curves. Larger quantities of RNA duplexes were prepared in a manner similar to that described above for thermally induced melting studies. A greater effort was made to ensure a 1:1 molar ratio of complimentary strands. Transcription reactions were scaled up to 100 μL or 1 mL volumes. After transcription, the DNA templates were digested with DNase A, and the reaction mixture was extracted with phenol−chloroform twice and then with chloroform alone. The relative amounts of the two transcripts needed to give a 1:1 molar ratio were determined by

titrating a given amount of the forward transcript with varying amounts of the reverse transcript. The samples were mixed, heated, and cooled as described above and then run on a 6% PAG to determine the ratio which would produce only the dsRNA band. Equimolar amounts of forward and reverse transcripts were then mixed, heated, and cooled.

Approximately 200 μL of prepared RNA duplex ($\sim$0.5 μg/μL) was diluted with 2 mL of 0.5 M NaCl + 5 mM NaH_2PO_4, 0.5 mM EDTA, pH 7.0, and concentrated to about 200 μL by centrifugation at 400 rpm using a Centricon-100 filter unit (Amicon). The Centricon-100 unit was chosen to remove any residual single-stranded (ss) RNA as well as smaller molecules. A 2 mL portion of 0.1 M NaCl was then added and the sample was concentrated again. This procedure was repeated three times to remove residual phenol/chloroform and rNTPs. The final volume of the RNA sample was adjusted to 200 μL by adding 0.1 M NaCl (pH 7.0) or the desired solvent.

Cuvettes for the melting study were thoroughly rinsed with water which had been treated with DEPC and autoclaved. The solvent used in the RNA melting study was 0.05 M NaCl with 5 mM NaH_2PO_4 and 0.5 mM EDTA (pH 7.0). One milliliter of RNA sample was placed in the cuvette, degassed, and then overlaid with mineral oil. The instrument employed was a Varian DMS-300 spectrophotometer modified to digitally collect absorbance and temperature readings. A modified cuvette holder was heated by fluid from a thermostated fluid circulator. Sample temperature was monitored by a platinum resistance probe (Omega Inc., $\pm$0.1 °C) inserted in a solvent-containing cuvette in an adjacent position of the cuvette holder. The heating rate was 0.5 °C/min. Absorbance values were monitored at 268 nm where the hyperchromicity for melting G·C and A·U pairs is approximately equal. After the RNA sample had reached a temperature at which UV absorbance indicated it was fully melted, it was cooled down to room temperature. A second melting curve was obtained using the same heating rate. The close similarity between the first and second melting curves indicated that degradation was not significant.

The melting behavior of duplex RNA was calculated using a previously described algorithm developed for DNA duplexes (*17*). The model employed assumed that the stability of a base pair sequence depends on base pair doublet stacking interactions (*2*). Internal loop free energy parameters estimated from DNA studies were assumed (*17*), since values based on RNA duplexes are unavailable. RNA base pair stacking parameters were extrapolated from thermodynamic parameters determined with RNA oligomers in 1 M NaCl (*3*). A T_{MN} value for each base pair doublet in 1 M Na^+ was obtained by dividing the stacking enthalpy change by the entropy change. These values were then extrapolated to 0.05 M Na^+ using values of $dT_m/d(\log [Na^+])$ estimated from periodic sequence RNA melting curves. Studies of poly(rA)·poly(rU) and poly(rAU)·poly(rAU) give values of about 19.5 °C for $dT_m/d(\log [Na^+])$ (*18*), whereas studies of poly(rG)·poly(rC) and poly(rGC)·poly(rGC) give a value of 13. (*18*). For base pair doublets with only A·U pairs or one A·U and one G·C pair, we assumed 19.5 for $dT_{MN}/d(\log [Na^+])$. A value of 13 was employed for base pair doublets with only G·C pairs. Although some of the parameters employed for the calculation are based on questionable assumptions (e.g., the linearity of $dT_m/d(\log [Na^+])$ from 1 m to 0.05 M Na^+ and a value of $dT_m/d(\log [Na^+]) = 19.5$ for A·U/G·C doublets), they provide a first-order approach given available data. Other values for the A·U/G·C doublets did not generate as good a fit with the experimental data.

Thermodynamic Analysis. For long DNA and RNA duplexes in which the first domain melts from an end in an all-or-none manner, leaving a partial duplex, the free energy change of the domain is given by

$$\Delta G = \Delta H - T\Delta S \qquad \text{(a)}$$

where ΔH is the domain enthalpy and ΔS the domain entropy. The melting of an individual domain is an intramolecular event and thus independent on the concentration of duplex molecules. The following relation holds for domain enthalpy and entropy:

$$\Delta H = T_m \cdot \Delta S \qquad \text{(b)}$$

If one to several base pair changes occur in the domain that do not alter the domain size, the free energy difference in melting the original (ΔG) and altered ($\Delta G'$) domains at temperature T will be linearly correlated to their melting temperature difference (δT_m). This is apparent from eqs a and b, assuming ΔS is essentially unchanged:

$$\delta\Delta G \equiv \Delta G' - \Delta G = T'_m \cdot \Delta S - T_m \cdot \Delta S = -\delta T_m \cdot \Delta S$$

This is eq 2 in the Results section.

Definition. Base pairs are denoted as GC, CG, AU, UA or G·C, C·G, A·U, U·A. A mismatch is defined as a base pair combination other than GC and AU. There are twelve such combinations in this study: AC, AG, AA, GA, GU, GG, UU, UG, UC, CA, CU, and CC. The first letter corresponds to the base in the forward strand of the RNA duplex, and the second letter to the base in the reverse strand.

RESULTS

RNA Duplexes. Figure 1a shows the 373 bp DNA region from which the RNA duplexes were transcribed. Primer-directed PCR mutagenesis was used to produce 19 DNA fragments with base pair substitutions at each of the six positions indicated with a down arrow. Sites at which specific base pair substitutions were previously available in plasmid DNAs (see Materials and Methods) are indicated by the filled triangles. Figure 1a also shows the primer pairs that were employed to produce 368 bp and 374 bp DNAs with the T7 RNA polymerase promoter sequence at one or the other end.

The RNA_f and RNA_r runoff transcripts from the forward and reverse DNA templates were hybridized to produce 345 bp RNA duplexes with 3′ overhangs of 6 bases on the *Eco*RI end (Figure 1b). By mixing appropriate pairs of RNA_f and RNA_r type transcripts, duplexes containing all possible base pair substitutions and mismatches were produced at positions −36, -35, −34, −33, −28, and −27. Table 1 shows the nearest neighbor base pairs at these six sites. A more limited number of base pair substitutions and mismatches were produced at sites −15, −12, and −5. Table 3 shows the nearest neighbor pairs at these three additional sites and the substitutions and mismatches examined.

Melting Curves. Denaturation or melting curves monitored by UV absorbance were obtained on several 345 bp RNA duplexes. Previous melting curve studies have shown that the 373 bp DNA fragment of Figure 1a has three melting

Table 1: Relative Stability Order of RNA Duplex with Base Pair Differences

position	relative stability order
−36[a]	1. GC > CG > AU > UA > GU > UG > GG = GA > AC═CA > AA = AG > UU = UC > CC = CU
GXU(AYC)	2. CG > GC > AU > UA > UG > GU > GA > GG > AG > CA = AC > AA > UU = UC > CU = CC
−35	1. GC > CG > AU > UA > GU > UG > GG > AC = GA = CA > AA = AG > UC = CU > UU = CC
GXU(AYC)	2. CG > GC > AU > UA > UG > GU > GA > GG > AG > CA = AC > AA > UU = UC > CU = CC
−34	1. CG > GC > AU > UA > GU > UG > GG > AC═CA > AA = AG = GA = CU = CC > UC > UU
UXU(AYA)	2. CG > GC > AU > UA > GU > UG > GG > GA > AG > AA > CA > AC > UU > UC═CU = CC
−33	1. GC═CG > AU = UA > UG = GU > GG > AA = AG = GA > AC = CA > UU = UC = CU = CC
UXA(UYA)	2. GC═CG > AU = UA > UG = GU > GG > AG = GA > AA > AC = CA > CC > UC = CU > UU
−28	1. CG > GC > AU = UA > UG > GU > AG = GG > AC > CA > AA = GA = CU > UU = UC═CC
UXC(GYU)	2. CG > GC > AU = UA > GU > UG > AG > GG > GA > AA > CA > AC > CU > UU = CC > UC
−27	1. CG > GC > AU = UA > UG = GU > GG > AC > AG = GA > AA = CA > UC═CU > UU = CC
CXU(AYG)	2. CG > GC > AU = UA > UG > GU > GG > AA > AG = GA > AC = UC > UU = CA > CC > CU

[a] XY represents a base pair combination, with X in the forward strand and Y in the reverse strand. Its position is indicated by number relative to Figure 1a. 1. Relative stability order determined by parallel TGGE; 2. relative stability order calculated using stacking parameter given by Serra and Turner[1] and the algorithm described in the text.

Table 2: Determination of Free Energy Differences Among RNA Duplexes Differing by Single Base Pairs and Mismatches

	−36 GXU[f]			−35 GXU			−34 UXU			−33 UXA			−28 UXC			−27 CXU		
	δT_μ[a]	$\delta\Delta G$[b]	$\delta\Delta G_{ST}$[c]	δT_μ	$\delta\Delta G$	$\delta\Delta G_{ST}$	δT_μ	$\delta\Delta G$	$\delta\Delta G_{ST}$	δT_μ	$\delta\Delta G$	$\delta\Delta G_{ST}$	δT_μ	$\delta\Delta G$	$\delta\Delta G_{ST}$	δT_μ	$\delta\Delta G$	$\delta\Delta G_{ST}$
AU	2.1	2.7	1.8	1.8	2.3	1.8	1.6	2.1	2.1	1.8	2.3	2.3	2.0	2.6	2.1	2.1	2.7	1.9
AA	4.7	6.1	4.7	4.7	6.1	4.7	3.6	4.7	4.7	3.4	4.4	4.5	4.7	6.1	4.7	4.2	5.5	3.9
AC	4.3	5.6	4.6	4.5	5.9	4.6	3.5	4.6	5.0	3.6	4.7	5.0	4.4	5.7	4.1	4.1	5.3	4.1
AG	4.7	6.1	4.5	4.3	5.6	4.5	3.5	4.6	4.6	3.4	4.4	4.3	4.4	5.7	4.9	4.1	5.3	4.0
UU	4.6	6.0	5.1	4.6	6.0	5.1	4.1	5.3	5.1	3.8	5.0	5.5	5.3	6.9	5.6	4.6	6.0	4.2
UA	2.0	2.6	2.0	1.9	2.5	2.0	1.8	2.3	2.3	1.9	2.5	2.3	2.3	3.0	2.0	2.1	2.7	2.0
UC	4.6	6.0	5.1	4.6	6.0	5.1	4.1	5.3	5.2	3.8	5.0	5.4	5.3	6.9	5.9	4.6	6.0	4.0
UG	3.3	4.3	2.6	3.1	4.0	2.6	2.9	3.7	3.7	2.9	3.5	3.7	3.6	4.8	3.6	3.3	4.3	3.4
GU	3.0	3.9	3.0	2.8	3.4	3.0	2.8	3.6	3.5	2.8	3.6	3.7	3.4	4.4	3.4	3.2	4.2	3.4
GA	4.2	5.5	4.2	4.2	5.5	4.2	3.7	4.8	4.4	3.3	4.3	4.3	4.6	6.0	4.4	4.2	5.4	4.0
GC	0.0	0.0	0.0	0.0	0.0	0.0	0.1	0.1	0.2	0.0	0.0	0.0	1.0	1.3	1.0	0.6	0.8	0.5
GG	4.2	5.5	3.9	4.0	5.2	3.9	3.4	4.4	4.3	3.3	4.3	4.1	4.0	5.2	4.2	4.0	5.2	3.8
CU	5.2	6.8	5.3	4.5	5.9	5.3	4.0	5.2	5.2	3.8	5.0	5.4	4.6	6.0	5.5	4.2	5.4	4.2
CA	4.6	6.0	4.6	4.2	5.5	4.6	3.8	4.9	4.8	3.5	4.6	5.0	4.3	5.6	4.8	4.6	6.0	4.6
CC	5.2	6.8	5.2	4.7	6.1	5.2	4.0	5.2	5.2	3.8	5.0	5.3	4.8	6.2	5.6	4.6	6.0	4.5
CG	0.3	0.4	−0.1	0.3	0.4	−0.1	0.0	0.0	0.0	0.0	0.0	0.0	0.0	0.0	0.0	0.0	0.0	0.0
η/T_μ[d,e]	0.8/39.0			0.9/40.9			1.0/40.8			1.0/40.9			0.9/39.0			0.8/39.0		

[a] δT_μ, in degrees Celsius, is the transition temperature difference determined by perpendicular TGGE. [b] $\delta\Delta G$ is the free energy difference in kilocalories/mole from δT_μ. The uncertainty is ±15%. [c] $\delta\Delta G_{ST}$ is the calculated free energy difference using data provided by Serra and Turner[1] in kilocalories/mole. [d] η is $\langle\delta\Delta G_{ST}\rangle/\langle\delta\Delta G\rangle$, the slopes of the lines from Figures 8 and 9. [e] T_μ is the average transition temperature for the reference RNAs in degrees Celsius. Reference RNAs have $\delta T_\mu = 0$. [f] The number refers to the central base and is referenced to the sequence positions of Figure 1a.

Table 3: Determination of Free Energy Differences for Positions −15, − 12, −5

	−15 GXG(CYC)			−12 UXU(AYA)			−5 UXU(AYA)		
	δT_μ[a]	$\delta\Delta G$[b]	$\delta\Delta G_{ST}$[c]	δT_μ	$\delta\Delta G$	$\delta\Delta G_{ST}$	δT_μ	$\delta\Delta G$	$\delta\Delta G_{ST}$
GC	0.0	0.0	0.0				0.0	0.0	0.0
AU	2.2	2.8	1.8	0.0	0.0	0.0	1.6	2.1	1.9
GU	3.2	4.2	3.3				2.8	3.6	3.3
AC	4.8	6.2	4.3				3.2	4.2	4.8
UA				0.0	0.0	0.2			
AA				2.4	3.1	2.6			
UU				2.6	3.4	3.0			
η/T_μ	0.7/39.0			0.7/39.0			1.0/39.0		

[a] δT_μ is transition temperature difference determined by TGGE in degrees Celsius. [b] $\delta\Delta G$ is free energy difference from δT_μ in kilocalories/mole. [c] $\delta\Delta G_{ST}$ is free energy difference using data provided by Serra and Turner (1995) in kilocalories/mole. [d] See Table 2 for definitions of other symbols.

domains (*19*). From an analysis of the DNA derivative melting curve the first melting domain is ∼52 bp (±7%) at the *Eco*RI end, the second domain is the adjacent ∼65 bp, and the final domain was the remaining 253 bp. On the basis of the similar stability differences between dG·dC and dA·dT vs rG·rC and rA·rU base pairs, it was anticipated that a RNA duplex with this region's sequence would exhibit similar melting domains. Results shown in Figure 2 confirmed this hypothesis. The melting curve of the 345 bp RNA duplex with the −5AU sequence is shown. Two small subtransitions are observed followed by one large subtransition. Similar transition curves were observed with other RNA duplexes in the 0.05 M Na^+ solvent. Melting curves in a 0.5X TBE solvent also showed three step transitions but at lower temperatures (not shown).

The number of base pairs contributing to each melting step in Figure 2 was estimated from the derivative of the melting curve. The relative area of each peak in the derivative melting curve was calculated. The first subtransition corresponded to ∼54 bp (±10%), the second subtransition corresponded to ∼60 bp, and the last step contained the remainder of the molecule. A theoretical melting curve of the RNA sequence, based on the model described in Materials and Methods, is also shown in Figure 2. Good overall agreement was observed. The agreement suggests that the theoretical curve can provide a useful interpretion of the melting curve. The calculated stability distribution of the RNA sequence, i.e. the effective T_m of each base pair or "melting profile" (*6*), indicates that the first subtransition

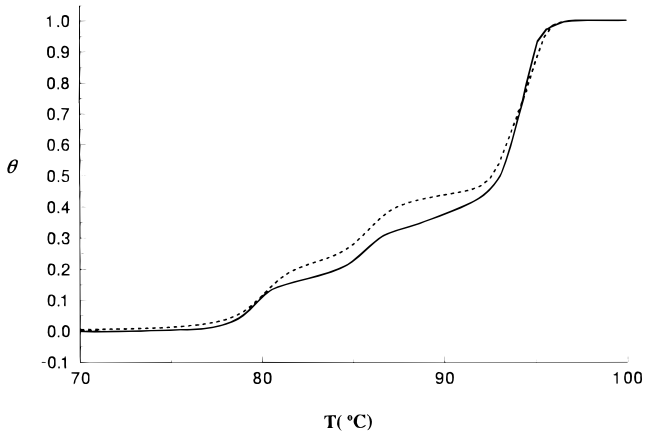

FIGURE 2: Comparison of experimental and predicted melting curve of a RNA duplex in 0.05 M Na^+. θ is the fraction of duplex unwound, and *T* is the temperature. The solid curve is the smoothed experimental melting curve of the 345 bp RNA −5AU, (A•U pair at position −5). The dotted curve is the predicted melting curve of this RNA.

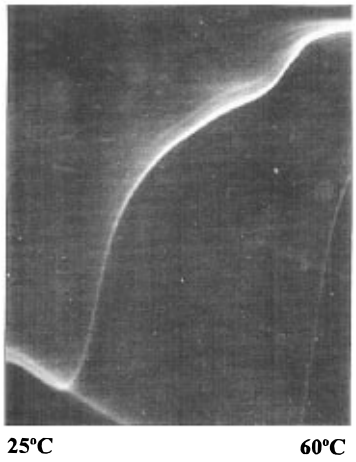

FIGURE 3: Perpendicular temperature gradient gel showing the mobility curve of the RNA −5AU. The temperature gradient was from 25 to 60 °C and the gel was run at 120 V for 12 h.

corresponds to the ∼54 bp segment at the *Eco*RI end of the molecule, the second subtransition results from the adjacent ∼60 bp, and the final subtransition corresponds to the remaining ∼233 bp. Independent results described below are consistent with the above location and size of the first melting domain.

TGGE Mobility Transition. Perpendicular TGGE experiments display a temperature-induced mobility transition of duplex nucleic acid molecules (*19, 20*). Figure 3 shows the mobility transition of the 345 bp RNA with A•U at −5 for the temperature range of 25−60 °C. The initial linear increase in mobility of the RNA with temperature is also observed with DNA duplexes (*8, 19*) and is due to the effect of temperature on gel viscosity and/or pore size.

Previous analyses of DNA electrophoretic retardation accompanying partial melting in a polyacrylamide gel (*8, 21*) employed the equation

$$\mu(T) = \mu_o \exp[-p(T)/\mathrm{L}] \qquad (1)$$

where $\mu(T)$ is the mobility of the partially melted molecule at temperature *T*, μ_o is the mobility of the fully intact duplex. *L* is referred to as the "length of the flexible unit" of a single strand in number of nucleotides (*21*), and $p(T)$ is the average

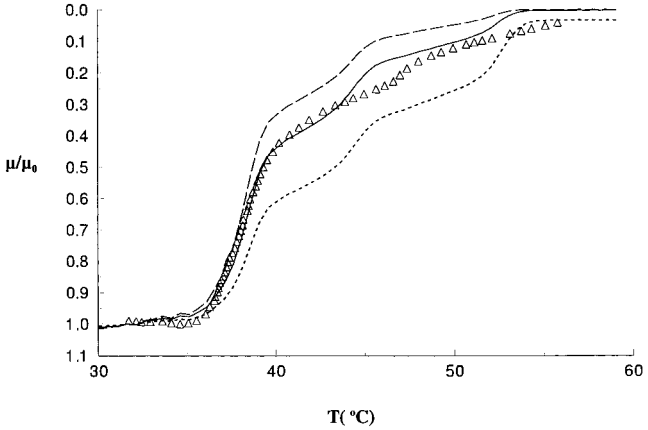

FIGURE 4: Comparison between normalized mobility curve of the RNA −5AU from Figure 3 and three predicted mobility curves calculated from eq 1. The experimental curve is indicated by triangles. The dotted, solid, and dashed curves correspond to predictions with L = 100, 60, and 45, respectively. Normalization procedure for experimental curve and parameters for calculation are described in text.

number of melted base pairs at temperature *T*. We assumed this equation applies to RNA duplexes. Figure 4 compares three calculated mobility curves of the 345 bp RNA with A•U at −5 using eq 1 with the normalized experimental curve ($\mu(T)/\mu_o$). The three calculated curves used *L* values of 45, 60, and 100 with $p(T)$ vs *T* determined from the normalized UV melting curve of Figure 2. The temperatures of $p(T)$ vs *T* curve from the UV melting data were uniformly lowered by 42 °C. This shift was made to compensate for the influence of the gel's urea−formamide denaturant and lower ionic strength.

Figure 4 shows that a value of $L = 60$ produced a good fit to the first mobility step of the experimental curve ($1.0 > \mu/\mu_o > 0.4$). This correspondence implies that unwinding of the RNA's first melting domain is responsible for the first mobility step. The second and third melting steps predicted by the $L = 60$ curve closely track the experimental curve but do not completely match the broader features of the experimental transition. The discrepancy may be due to several factors, including the inadequacy of eq 1 and/or experimental artifacts at the higher temperatures. Since the top of the gel was slightly above the heating plates, molecules at the higher temperature end initially migrated in a less denatured state than the location dictated. The perpendicular TGGE experiments described below employed temperature gradients that focused on the first mobility step.

Parallel TGGE. Figures 5 and 6 show examples of parallel TGGE experiments on RNA duplexes. All base pair changes and mismatches are shown for positions −34 and −27. The temperature gradient of 40−45 °C enabled all RNAs to be observed in one gel. Greater separation of the mismatched RNAs was obtained by increasing the run time and/or decreasing the temperatures by several degrees (*7*). Similar results were obtained for all base pair changes and mismatches at positions −36, −35, −33, and −28 (not shown). We note that the RNA bands in the parallel gels appear to be closely spaced doublets. We are uncertain of the origin of this phenomena. It may come from the heterogeneity in duplex ends due to T7 transcription. Providing that a consistent method was used to measure the band depths, it did not effect the analysis. The order of stability for all base pairs and mismatches at each of the six

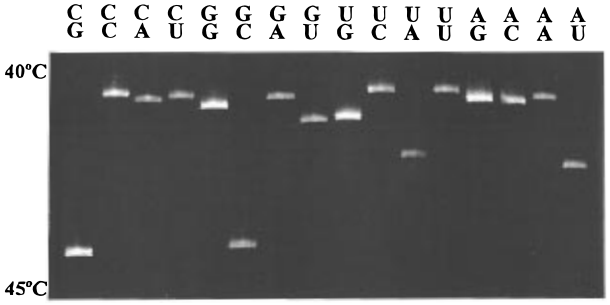

FIGURE 5: Parallel TGGE experiments of RNA duplex with base pairs or mismatches as indicated at position −34. The temperature gradient was from 40 to 45 °C. Samples were run at 120 V for 12 h.

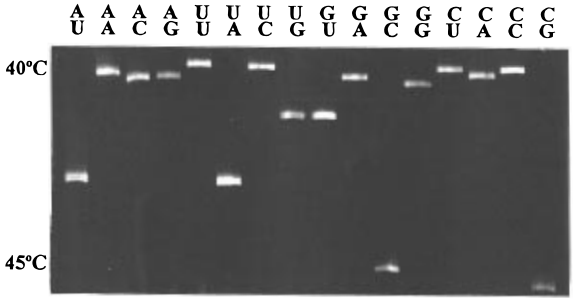

FIGURE 6: RNA duplexes with base pairs or mismatches as indicated at position −27. The electrophoresis conditions were the same as in Figure 5.

positions is given in Table 1 by the rows numbered "1." The rows numbered "2." in Table 1 are described below.

The different orders of stability at the various positions described in Table 1 indicate that the stability of a base pair or mismatch is influenced by its identity and nearest neighbors. Some trends are observed. A G·U pair is more stable than all other single mismatches at all positions. This result differs from an analogous comparison of G·T with other mismatched bases in DNA (*7*). In addition, mismatches containing at least one purine base are more stable than those containing two pyrimidine bases.

Base changes at positions −36 and −35 have the same nearest neighbors (5′-GXU-3′) but different second neighbors. The sequence surrounding position −36 is 5′-AGXUU-3′, while the sequence surrounding position −35 is 5′-GGXUU-3′. RNA duplexes with base pair substitutions at these two sites had the same order of separation (G·C>C·G>U·A> A·U). However, the order of separation of the mismatches differed. For changes at position −36, the heirarchy of stability for the mismatches was GU>UG>GG = GA>AC = CA>AA = AG>UU = UC>CC = CU. For changes at position −35, the heirarchy of stability was GU>UG>GG>AC = CA = GA>AA = AG>UC = CU>CC = UU. This result indicates that second neighbor base pairs can influence the stability of mismatches in RNA.

The sequence surrounding position −33 is 5′-UUXAA-3′. Due to the symmetric nature of this site, one expects that the RNA duplex with paired bases X·Y at position −33 will have the same stability as the RNA with paired bases Y·X at this position, assuming no interactions beyond second neighbor. As indicated in Table 1, this expectation was observed, i.e. −33AC = −33CA, −33AG = −33GA, −33AU = −33UA.

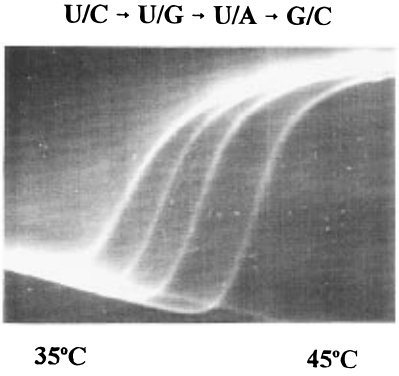

FIGURE 7: Perpendicular temperature gradient gel of four RNA duplexes differing by a single base pair or mismatch at position −36. The temperature gradient was 35 to 45 °C and shows the mobility change of only the first melting domain of the RNAs. The transitions from left to right correspond to RNAs with the following pair of bases at position −36: U/C, U/G, U/A and G/C.

Perpendicular TGGE. Perpendicular temperature gradient gels were used to determine mobility transition temperatures (T_μ) of the first melting domain of the RNA molecules. Figure 7 shows a typical perpendicular TGGE experiment in which four RNA duplexes are run simultaneously. The assignment of a transition curve to a RNA molecule was made on the basis of the relative RNA stabilities determined by parallel TGGE. T_μ was defined as the midpoint temperature of the domain's mobility transition curve. Each mobility curve was determined from the linearly extrapolated initial mobility decrease and final mobility increase as baselines.

In each experiment such as Figure 7, the most stable RNA, with either G·C or C·G at the position under investigation, was used as an internal reference. Transition temperatures for each RNA were measured and the difference in transition temperature for each fragment vs the common reference (δT_μ) was determined. The standard deviation of T_μ measurements was about ±0.5 °C upon repeated experiments. δT_μ values were reproducable to ±0.2 °C or less. The reference RNA for experiments at positions −36 and −35 had a G·C at the position being investigated. For experiments involving positions −34, −33, −28, and −27, the reference RNA had a C·G at the position being studied. Table 2 summarizes the measurements of δT_μ for the above six positions. Table 3 summarizes the more limited data obtained at positions −15, −12, and −5. The $\delta T_\mu'$ s ranged from 0−1 °C for an RNA with a G·C ↔ C·G substitution, from 1 to 2 °C for a G·C to A·U or U·A substitution, from 2 to 3 °C for a change from G·C to G·U or U·G, and from 3 to 5 °C for a substitution by mismatched bases. $\langle T_\mu \rangle$ values of the reference RNAs are in the last row of Tables 2 and 3.

Free Energy Analysis. The full unwinding transition of the 345 bp RNA monitored by UV absorbance in solution (Figure 2) as well as gel mobility (Figure 4) indicate that the first melting domain can be treated as a separate transition. The analysis in Materials and Methods shows that the transition's temperature difference caused by a base pair change in the first domain can be related to a corresponding free energy difference (*8*, *22*). The free energy difference, $\delta\Delta G$, between a reference RNA and an RNA differing by a single base pair change is given by

$$\delta\Delta G = -\Delta S \delta T_m \qquad (2)$$

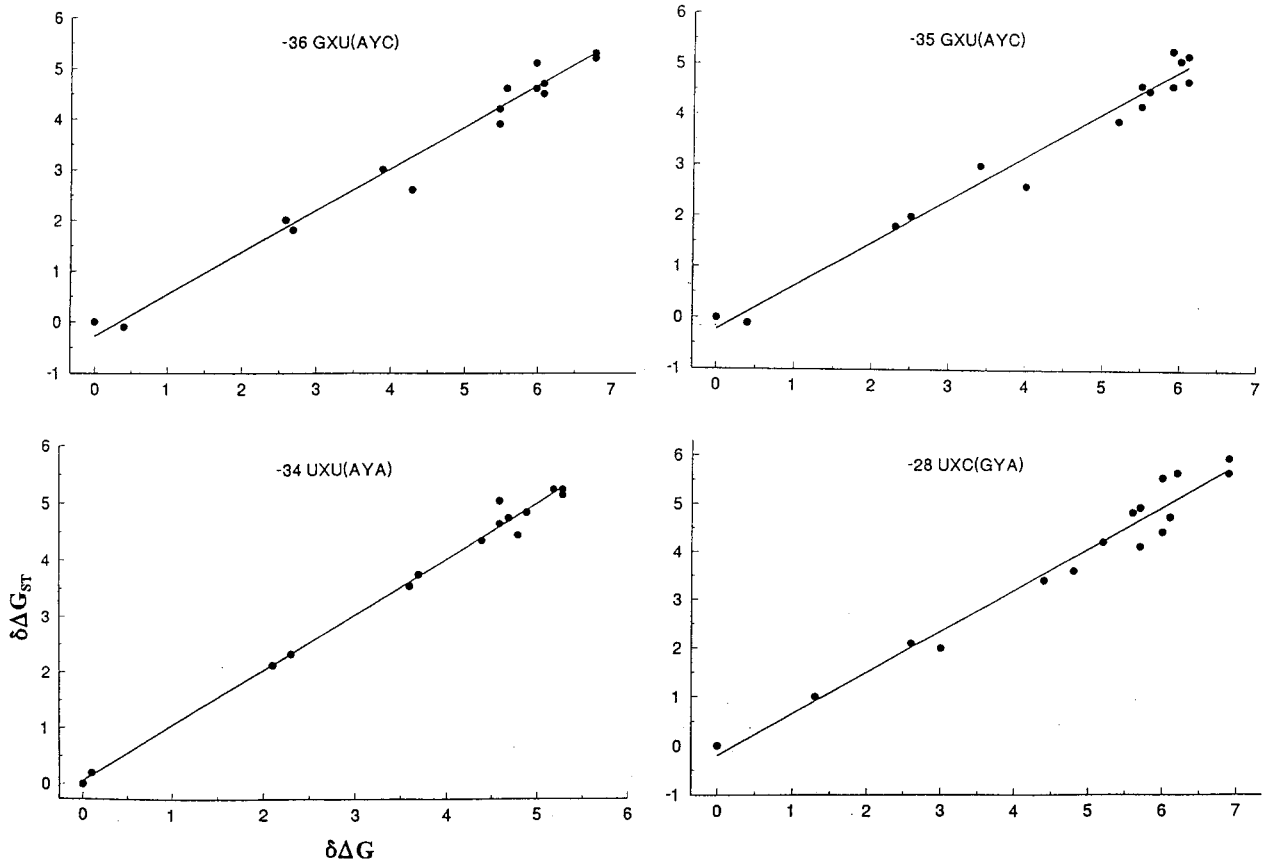

FIGURE 8: Plots of experimental $\delta\Delta G$ vs the calculated $\delta\Delta G_{ST}$ from data in Table 2 at positions, −36, −35, −34, and −28. For each plot, the x-axis represents $\delta\Delta G$ and the *y*-axis $\delta\Delta G_{ST}$.

ΔS is the entropy change for unwinding the first domain, and δT_m is the shift in T_m due to the base pair change. Assuming that $\delta T_m \approx \delta T_\mu$, one has a linear relationship between δT_μ and the free energy difference due to a base pair or defect substitution. ΔS can be estimated by multiplying the number of base pairs in the first melting domain, N_1, by $\langle\Delta S°\rangle$, the average entropy change/base pair stacking interaction. Analysis described earlier indicated that $N_1 \approx 54 \pm 5$ bp. No previous estimates exist for $\langle\Delta S°\rangle$ under the solvent conditions of the temperature gradient gel. We assumed the $\langle\Delta S°\rangle$ value determined from RNA oligomer studies in 1 M NaCl (*1*), 25 cal/°K mol, to estimate $\delta\Delta G$ for the RNA pairs examined. These values are listed in Tables 2 and 3. The uncertainty in $\delta\Delta G$ values based on measurement error in δT_μ and N_1 is about 15%.

It is of interest to compare the $\delta\Delta G$ values with values calculated from the extensive set of empirically based free energies for RNA base pair doublets, terminal mismatches, and G·U pairs compiled by Serra and Turner (*1*). We note that the latter values were determined from melting transitions of RNA oligomers in 1 M NaCl, a solvent very different than that used in TGGE. As mentioned earlier, Table 1 shows that the stability of an internal mismatch is dependent on the identity of the mismatch as well as its nearest neighbor context. Due to a lack of data, Serra and Turner (*1*) employed a rule for the free energy contribution of single internal mismatches that was independent of their identity and context. We propose a modification of this rule that uses their data on terminal mismatches.

For two base pairs sandwiching a mismatch X·Y, for example (GXU)·(AYC), we assume the free energy can be written as

$$\Delta G = \Delta G_{GX(YC)} + \Delta G_{XU(AY)} + \Delta G_{loop} \qquad (3)$$

where $\Delta G_{GX(YC)}$ and $\Delta G_{XU(AY)}$ are the stacking energies for the terminal mismatches. ΔG_{loop} is the free energy penalty for closing an internal loop with a base pair. If X·Y is closed by two G·C base pairs, we assume $\Delta G_{loop} = 0.8$ kcal/mol. If X·Y is closed by one G·C and one A·U, then $\Delta G_{loop} = 1.6$ kcal/mol, and if X·Y is closed by two A·U's, $\Delta G_{loop} = 2.4$ kcal/mol. For the example triplet (GAU)·(ACC) at 37 °C, the terminal mismatch free energies are $\Delta G_{GA(CC)} = -1.5$ kcal/mol, and $\Delta G_{AU(AC)} = -0.6$ kcal/mol. From the above algorithm, $\Delta G_{loop} = 1.6$ kcal/mol, and eq 3 gives $\Delta G_{(GAU)\cdot(ACC)} = -0.5$ kcal/mol. Free energy increments of G·U mismatches were treated differently. The stacking energies for terminal G·U's from Serra and Turner (*1*) were used, but 0.8 kcal/mol was employed for ΔG_{loop} independent of the closing base pairs.

Free energy differences for all pairs of RNAs differing by a base pair or mismatch were calculated using the above algorithm for mismatches, and the base pair stacking data of Serra and Turner (*1*). These values are listed as $\delta\Delta G_{ST}$ in Tables 2 and 3 and were plotted against the $\delta\Delta G$ values determined from eq 2 for the nine positions examined. Figure 8 shows the correlations found for all base pair changes and mismatches at positions −36, −35, −34, and −28. Linear correlations of similar quality were observed for the positions −33 and −27, as well as positions −15, −12, and −5, where a more limited set of data was collected (not shown). The slopes of the lines that best fit the data were close to 1 in all cases. The slope values are listed in Tables 2 and 3 under the column $\delta\Delta G_{ST}$. The general agreement supports the assumption that $\langle\Delta S°\rangle \approx 25$ cal/K

mol for the TGGE conditions. Differences from a slope of 1 may reflect solvent effects at specific sequences. The hierarchy of stability of each RNA duplex predicted from the 1.0 M NaCl data is listed in the rows numbered "2." of Table 1. The predicted heirarchy is similar to the observed heirarchy from the TGGE experiments but with some variation.

DISCUSSION

Tables 1−3 provide information on the order of stabilities for RNA base pair substitutions and mismatches in six different nearest neighbor environments. The results show that the relative stability of a mismatch within a RNA duplex depends on both its identity and its nearest neighbor context. This is consistent with the structural variations observed in studies of tRNAs (*23*) and short RNA oligomers (*24*, *25*) that show mismatched bases with different H-bonding patterns and stacking interactions with neighboring bases. The free energy parameters deduced from the current study should enhance the accuracy of RNA secondary structure predictions.

TGGE provides a new approach to evaluate the relative free energies of bulges, mismatches, and loops within a RNA duplex. In the current work the free energies of single mismatches were determined from the mobility transition temperatures of the first melting domain of a RNA fragment with and without the mismatch. An important assumption for employing eq 2 is that the size of the domain does not change with the introduction of the mismatch. Evidence supporting this assumption comes from the perpendicular TGGE experiments. The mobility transition curves were nearly parallel for the RNAs with base pairs or mismatches at a given site. Substitution of mismatches for base pairs did not significantly change the melting cooperativity within the melting domain.

Results from Table 1 show that mismatches containing one or two purines are more stable than mismatches with only pyrimidines. This may be explained in part by hydrogen bonds involving purine−purine or purine−pyrimidine bases, as observed in single mismatches such as A·C, and A·G (*26*). Two pyrimidine bases in a single mismatch are less likely to bond with each other. However, hydrogen bonding of U·U has been found in tandem mismatches (UU)·(UU) (*4*, *26*) and detected by Wang et al. in a hairpin stem (*27*). Another factor expected to enhance the stability of purine mismatches is their stacking interactions with neighboring base pairs. Previous studies on unpaired terminal nucleotides show that base identities have little influence on the stacking energies of the 5′ unpaired nucleotides but a large effect on the 3′ unpaired nucleotides (*3*). On average, the stacking energies of 3′ unpaired purine bases are about 0.6 kcal/mol more stable than those of pyrimidine bases.

Previous studies indicate that the nearest neighbor model can generally predict the free energies of RNA duplexes at 37 °C with Watson−Crick type base pairs (*3*). For certain sequences, however, second neighbor interactions or other factors result in greater discrepancies. There is little previous data on how second neighbor base pairs effect the stability of single mismatches. A study of two G·A mismatches in an eight bp RNA helix suggested that a mismatch may induce a distortion that extends to its second neighbors (*5*). A comparison of our data at positions −35 and −36 shows that for this sequence a single mismatch has a measurable but small second neighbor effect.

The melting behavior of the 345 bp RNA duplexes reported in this work share similarities with that of their analogous DNA molecules (*7*). For example, DNA single mismatches with two pyrimidine bases were usually less stable than the mismatches containing purine bases, as observed for the RNAs. The 373 bp DNA template has three melting domains, as does the somewhat shorter RNA duplex. The δT_μ's for the RNAs and thus the $\delta\Delta G$'s in this study were linearly correlated with predicted free energy differences calculated from RNA oligomer parameters (i.e., Figure 8). A similar correlation is observed between δT_μ values determined from the analogous DNA duplexes differing by base pair substitutions, and free energies predicted from DNA oligomer data from SantaLucia et al. (*27*, *28*) (Johnson, Zhu, and Wartell unpublished).

A difference in the mobility behavior of the RNA and DNA molecules was noted in the analysis of the perpendicular TGGE mobility profiles. The RNA duplex showed a larger decrease in mobility for the first melting domain than was observed for the related but longer DNA fragment (*7*). Using the same gel conditions (0.5X TBE with 58% denaturant) the DNA mobility curve required an L value of 100 in order for eq 2 to match the mobility transition. Figure 4 shows that an L value of 60 best fits the RNA curve. A comparison of the DNA melting transition (*7*) and the current RNA results indicate that the first melting domains of the DNA and RNA are very similar in size. The parameter L has been described as a "length of the flexible unit" of the single strand (*20*). Although L is expected to be related to the "stiffness" or persistence length of the single strands, it may also be related to the charge density of the polynucleotide and/or the ratio of the melted and duplex regions. We have observed that the mobility profile of the first melting domain of a 345 bp RNA·DNA hybrid of the above sequence is more similar to the profile of the 345 bp RNA than the 373 bp DNA (unpublished results). Additional studies with homologous DNA, RNA, and RNA·DNA hybrids are needed to determine what factors have the strongest influence on the value of L.

ACKNOWLEDGMENT

We wish to thank Ted Johnson, for assistance with PCR, and Shashi Poddar, for RNA melting curve calculations in the early phase of the work.

REFERENCES

1. Serra, M. J., and Turner, D. H. (1995) *Methods Enzymol. 259*, 242−261.
2. Freier, S. M., Kierzek, R., Jaeger, J. A., Sugimoto, N., Caruthers, M. H., Neilson, T., and Turner, D. H. (1986) *Proc. Natl. Acad. Sci. U.S.A. 83*, 9373−9377.
3. Turner, D. H., Sugimoto, N., and Freier, S. M. (1988) *Ann. Rev. Biophys. Chem. 17*, 167−192.
4. Wu, M., McDowell, J. A., and Turner, D. H. (1995) *Biochemistry 34*, 3204−3211.
5. Morse, S. E., and Draper, D. E. (1995) *Nucleic Acids Res. 23*, 302−306.
6. Ke, S. H., Kelly, P. J., and Wartell, R. M. (1993) *Electrophoresis 14*, 561−569.

7. Ke, S. H., and Wartell, R. M. (1994) *Nucleic Acids Res. 21*, 5137−5143.
8. Ke, S. H., and Wartell, R. M. (1996) *Nucleic Acids Res. 24*, 707−713.
9. Ke, S. H., and Wartell, R. M. (1995) *Biochemistry 34*, 4593−4599.
10. Zuker, M. (1989) *Science 244*, 48−52.
11. Zuker, M., Jaeger, J. A., and Turner, D. H. (1991) *Nucleic Acids Res. 19*, 2707−2714.
12. Tatti, K. M., and Moran, C. P., Jr. (1984) *J. Mol. Biol. 175*, 285−297.
13. Wartell, R. M., Hosseini, S. H., Moran, C. P., Jr. (1991) *Nucleic Acids Res. 18*, 2699−2705.
14. Clark, J. M. (1988) *Nucleic Acids Res. 16*, 9677−9686.
15. Sambrook, J., Fritsch, E. F., and Maniatis, T. (1989) *Molecular Cloning: A Laboratory Manual, 2nd ed., Cold Spring Harbor Laboratory Press*, Cold Spring Harbor, N.Y.
16. Cazenave, C., Uhlenbeck, O. C. (1994) *Proc. Natl. Acad. Sci. U.S.A. 91*, 6972−6976.
17. Wartell, R. M., and Benight, A. S. (1985) *Physics Rep. 126*, 67−107.
18. Klump, H. (1990) in *Landolt-Bornstein New Series VII, Volume 1c, Nucleic Acids*, pp 241−256, Springer Verlag Inc., Berlin.
19. Wartell, R. M., Hosseini, S. H., Powell, S., and Zhu, J. (1997) *CRC Series of Analytical Biotechnology−Genome Analysis*, in press.
20. Reisner, D., Henco, K., and Steger, G. (1991) in *Advances in Electrophoresis* (Chrambach A., Dunn, M. J., and Radola, B. J., Ed.) pp 169−250, VCH Pub., New York.
21. Lerman, L. S., Fisher, S G., Hurley, I., Silverstein, K., and Lumelsky, N. (1984) *Annu. Rev. Biophys. Bioeng. 13*, 399−423.
22. Woodson, S. A., and Crothers, D. M. (1987) *Biochemistry 26*, 904−912.
23. Kim, S. H., Suddath, F. L., Quigley, G. J., McPherson, A., Sussman, J. L., Wang, A. M. J., Seeman, N. C., and Rich, A. (1974) *Science 185*, 435−440.
24. Walter, A. E., Wu, M., and Turner, D. H. (1994) *Biochemistry 33*, 11349−11354.
25. Wu, M., and Turner, D. H. (1996) *Biochemistry 35*, 9677−9689.
26. SantaLucia, J., Jr., Kierzek, R., and Turner, D. H. (1991) *Biochemistry 30*, 8242−8251.
27. Wang, Y. X., Huang, S., and Draper, D. E. (1996) *Nucleic Acids Res. 24*, 2666−2672.
28. SantaLucia, J., Jr., Allawi, H. T., and Senneviratne, P. A. (1996) *Biochemistry 35*, 3555−3562.
29. Allawi, H. T., and SantaLucia, J., Jr. (1997) *Biochemistry 36*, 10581−10594.

BI9716783